Mapping of **b***-values, earthquake relocation, and Coulomb stress changes during 1992–2007 in the Murindó seismic zone, Colombia*

Viviana Dionicio & John J. Sánchez

Journal of Seismology

ISSN 1383-4649

J Seismol
DOI 10.1007/s10950-011-9263-6

Springer

J Seismol
DOI 10.1007/s10950-011-9263-6

ORIGINAL ARTICLE

Mapping of *b*-values, earthquake relocation, and Coulomb stress changes during 1992–2007 in the Murindó seismic zone, Colombia

Viviana Dionicio · John J. Sánchez

Received: 24 September 2010 / Accepted: 1 December 2011

Abstract Seismicity in the Murindó seismic zone, Colombia (6° to 8° and −75.5° to −78.0°) during 1992–2007 included the occurrence of the M_W 6.6 foreshock on October 17, and M_W 7.1 mainshock on October 18, 1992, and aftershocks, which caused severe damage throughout the region. We modeled this seismic sequence by means of Coulomb stress changes imparted by slip along two semi-vertical fault planes with left-lateral motion and subdivided slip. Seismicity thereafter (1993–2007) was characterized by earthquakes magnitude in the range 0.7−6.1 for which a magnitude of completeness $M_C = 2.7$ was determined. *b*-values are relatively high to the south of the study region and relatively low to the north and northwest. The relocation of epicenters indicates that recent seismicity may be occurring on a fault that is yet to be mapped under the Atrato river valley. We conclude that the 1992 seismic sequence was a case of a major earthquake facilitated by the stress changes imparted during a strong rupture the previous day and that the aftershocks and background seismicity in the region can be explained by static Coulomb stress changes up to 50.1 bar. Our results have implications for hazard in Colombia and serve as basis to foster future investigations.

Keywords Colombia · *b*-values · Coulomb stress changes · Seismic hazard

V. Dionicio(✉)
INGEOMINAS-Red Sismológica Nacional de Colombia (RSNC), Bogotá, Colombia
e-mail: vivianadionicio@gmail.com

J. J. Sánchez
Departamento de Geociencias, Universidad Nacional de Colombia-Sede Bogota Edificio Manuel Ancízar, Bogota, Colombia
e-mail: jjsancheza@unal.edu.co

1 Introduction

Colombia has many seismogenic regions mainly associated with processes of crustal deformation and subduction. The focus of this study is the interaction among faults by means of static Coulomb stress changes in the region enclosed by 6°to 8° and −75.5° to −78.0°, known as the Murindó seismic zone (Fig. 1). The motivations of this paper include the occurrence of the 17–18 October, 1992 seismic sequence (M_W 6.6−7.1) and the time-varying microseismicity thereafter, particularly during 2003–2007. The 1992 seismic sequence caused severe damage in the region and spawned felt reports throughout Colombia.

Currently there is evidence supporting the hypothesis that faults interact among them by means of stress transfer in highly variable time scales of minutes to years. The static stress transfer studies

Published online: 07 March 2012

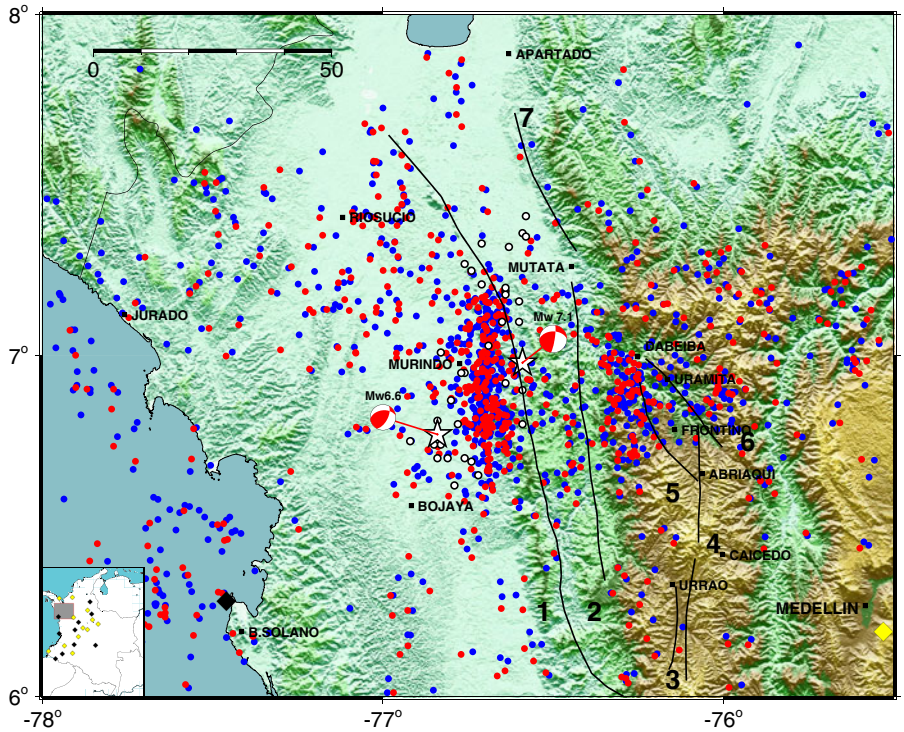

Fig. 1 Map of northwestern Colombian showing the distribution of epicenters used in this study. Blue circles: Earthquakes detected and located by Red Sismológica Nacional de Colombia (RSNC) between 1993–2006 with local magnitudes between 0.7 – 7.3. Red circles: Earthquakes relocated with HYPODD (Waldhauser 2001) between 1993–2006. White symbols (stars and dots): Epicenters of the 1992 seismic sequence relocated with JHD (Arvidsson et al 2002) with their focal mechanisms (GCMT 2008). Black squares: Towns and villages. Main faults (Gómez et al 2007; Paris et al 2000) are indicated by solid black lines and numbered as follows: 1, Murindó; 2, Murrí; 3, Urrao; 4, San Ruperto; 5, Abriaquí; 6, Cañasgordas; and 7, Mutatá. Black diamonds: Broad band seismograph stations. Yellow diamonds: Short period stations.

can help explain triggering of earthquakes on adjacent faults as well as aftershocks along the same fault. Along the same lines, static stress changes can also explain variations of seismicity rates in a region. Seismicity in northwestern Colombia and the 1992 seismic sequence have been the subject of study in a number of publications (Ammon et al 1994; Arvidsson et al 2002; Li and Toksöz 1993; Martinez et al 1994) that, respectively, reported the damage from the earthquakes, suggested possible models for the seismic source, and studied the seismotectonics of the region. Although the modeling of stress transfer have been successfully applied in many areas of the world and such modeling has become a sound tool in the assessment of seismic hazard for many countries, there are not many publications on this topic in Latin America (Lin et al 2000) and specifically in Colombia. In this work we study the Murindó seismic zone and the modeling of Coulomb static stress changes in nearby areas caused by dislocation along a master fault. To that end we perform a spatial-temporal descriptive analysis of shallow seismicity (depth < 40 km) in northwestern Colombia, characterizing the seismogenic zone by its earthquake productivity, magnitudes range, frequency of occurrence, b-value and relocation of epicenters using the double difference method (Waldhauser

2001). Additionally we construct a model of the seismic source in the Murindó zone hypothetical fault planes whose configurations are base on published studies on seismicity, source mechanisms and the geology and seismotectonics of the region (Arvidsson et al 2002; Gómez et al 2007; Martinez et al 1994). We test the hypothesis that dislocation along the south part of the master fault during the 1992 sequence changed the stress state to the north of the area and throughout the nearby regions where important faults such as Murindó, Murrí, Mutatá, Abriaquí and Cañasgordas have been documented. We surmise that the changes of stress imparted from the 1992 earthquakes influenced local seismicity.

2 Methods

2.1 Analysis of the earthquake catalog

We used the catalog of earthquakes located by *Red Sismológica Nacional de Colombia* (RSNC) between June 1993 and September 2007, within a region bounded by the coordinates 6°to 8° and −75.5° to −78.0°, down to a depth of 40 km. We used the computer program ZMAP (Wiemer 2001) to estimate the following seismic parameters:

- The frequency-magnitude distribution Eq. 1, the magnitude of completeness (M_C) and its temporal variation, and the average b-value for the entire study region,

$$\log N = a - b\,M, \tag{1}$$

  Where N is the cumulative number of earthquakes with magnitudes $\geq M$, and a and b are constants describing the productivity of a volume and the relative distribution of earthquakes sizes.
- The variation in seismicity rates in terms of the cumulative number of earthquakes versus time.
- Spatial variability of b-values throughout the region. Calculations were made based on a grid with nodes separation of 1 km, using the nearest 100 earthquakes around each node. To ensure the rigor in the mapping, we performed multiple tests by varying the grid nodes separation and the minimum number of earthquakes sampled around each node. We note that because of the intrinsic variability in detection sensitivity and magnitude determination for the different seismograph networks, the results of this work cannot be directly compared with other areas.

2.2 Relocation of earthquakes

We used the computer program HypoDD (Waldhauser 2001; Waldhauser and Ellsworth 2000) to relocate the epicenters determined by RSNC. The 1D velocity model used for earthquake location and relocation was derived by Ojeda and Havskov (2001) and is composed of 5 layers over a half space, with velocities increasing with depth. The basic input data are the differences in travel times for multiple pairs of earthquakes detected by a common station. An in-house program was developed to read the original files in Nordic format (Havskov and Ottemöller 2005) and write the appropriate HypoDD format. The reader is referred to the HYPODD manual (Waldhauser 2001) for further details on the technique and file formats.

2.3 Definition of a model for the 17–18 October, 1992, Murindó, precursory earthquake and mainshock

We established a model for the configuration and slip of the faults that ruptured during the sequence. In defining the model parameters we considered: Determinations of fault plane solutions reported by (GCMT 2008), locations of the seismic sequence by other researchers (Arvidsson et al 2002), the seismicity reported by RSNC following the sequence, field studies during the earthquakes, and available information on faults in the area (Cardona et al 2005; Cortés and Angelier 2005; Duque-Caro 1990; Paris et al 2000; Pulido 2003; Taboada et al 2000).

Epicenters of the 1992 seismic sequence were relocated by Arvidsson et al (2002) using Joint

Table 1 Relevant parameters for geometry of faults during the 1992 sequence

Earthquake (fault) modeled	Length (km)	Dislocation (m), left lateral motion	Depth (km)	Strike (°)	Dip (°)	Slip (°)
Precursory	30	0.53 to 0.74	20	28	60	55
Mainshock	70	1.26 to 1.56	20	9	81	46

Hypocenter Determination (JHD) (Dewey 1971). From the observed alignment of aftershocks, an empirical relationship between moment magnitude (M_W), the length of surface rupture, dislocation (Stein and Wysession 2003), and the focal mechanisms we incorporated the following relevant features in our model:

- For the orientation of the main fault we use the alignment of aftershocks from Fig. 1 in (Arvidsson et al 2002), suggesting a SW-NE trend.
- We use the strike, dip and slip computed by GCMT (2008) for precursory and main faults. In Table 1 we list the orientation for the faults that ruptured during the sequence.
- For the rupture length and of dislocation we use the empirical relations $M_W = 5.08 + 1.16 * log(SRL)$ and $log(AD) = -1.43 + 0.88 * log(SRL)$, where M_W is the moment magnitude, SRL is the surface rupture length in kilometers, and AD is the average dislocation in meters (Stein and Wysession 2003). Using $M_{Wprecursory} = 6.6$ and $M_{Wmainshock} = 7.1$, the relations give $SRL_{precursory} = 20.4$ km and $SRL_{mainshock} = 55.12$ km, respectively. These values seem to underestimate the likely actual lengths of the two faults. We use lengths of 30 km and 70 km as maximum values for the precursory and mainshock faults, consistent with earthquakes of magnitudes M_W of 6.8 and 7.2, respectively. For $20.4 \leq SRL_{precursory}(km) \leq 30$ and $55.12 \leq SRL_{mainshock}(km) \leq 70$, we obtain $0.53 \leq AD_{precursory}(m) \leq 0.74$ and $1.26 \leq AD_{mainshock}(m) \leq 1.56$, both with left lateral motion.
- For the width of the faults we consider shallow seismicity in the region by (RSNC), which occurs down to a depth of 20 km.

2.4 Computation of Coulomb stress changes

2.4.1 Orientation of regional stress

To determine the changes in Coulomb stress on optimally oriented faults we need to consider stresses that come from background regional tectonics. The study area is tectonically and geologically complex, and there are interactions among the Nazca, Caribbean, and South America plates. There have been several investigations on the nature of regional stresses (Cortés and Angelier 2005; Taboada et al 2000) in northwestern South America and our study area falls in the region where Cortés and Angelier (2005) suggest subhorizontal northwesterly regional compression. In Table 2 we list the suggested orientations for regional stress.

Table 2 Orientation of regional stress estimated by Cortés and Angelier (2005) for the study area

Region U (from Cortés and Angelier 2005)	σ_1		σ_2		σ_3	
	Strike (°)	Dip (°)	Strike (°)	Dip (°)	Strike (°)	Dip (°)
U_{com}	324	0	56	83	234	7

U_{com} = Compression in region U.

Table 3 Orientation of the main faults mapped in the region (Paris et al 2000; Gómez et al 2007)

Fault	Strike (°)	Dip (°)	Slip (°)
Murindó central	347.4	89	0
Murrí	1.4	89	0
Mutatá	326.4	70	0
Urrao	3.6	89	0
Cañasgordas	315.2	89	0

Table 4 Percent distribution of slip (lateral and reverse) for adjacent rectangles in the subdivided slip case

Test	Rectangle Number	Percent of total slip
A	4	80%
	others	2.5% each
B	5	80%
	others	2.5%each

2.4.2 Coulomb stress changes caused by the entire 1992 sequence

We use the software Coulomb 3.0 (Lin and Stein 2004; Toda et al 2005), our design for the ruptures includes modeling faults using two alternative configurations: **1)** Subdivided slip and **2)** Tapered slip. In the first case the fault is divided with an array of 9 rectangles of equal size. We number these rectangles from 1 to 9 starting with the southernmost and shallowest patch and progressing to the northernmost and deepest patch (see Fig. 4), in the second case we used 10 nested rectangles. In both cases we considered scenarios that involved rupture during the precursory event alone and during the entire sequence considering a cumulative effect. In each of the scenarios we computed Coulomb stress changes on: **1)** Specifically oriented faults (strike = 9°, dip = 81°, slip = 46°) for the precursory earthquake; **2)** Optimally-oriented strike-slip faults; and **3)** specifically oriented faults with configurations like the surrounding faults (Table 3) and the earthquakes with $M_W \geq 5.2$ reported in the GCMT catalog between 1994 and 2008 (Table 5), for the entire sequence.

Because the result did not dependent significantly on the dislocation model used (subdivided versus tapered fault), we show the results from the subdivided slip faults, in which case, the amount of slip in each of the rectangles was assigned as shown in Table 4. Briefly, the rectangle with most dislocation was represented as producing 80% of the total slip, and the remaining 20% was distributed equally among the other 8 rectangles. Two possible situations were considered: A) most of slip, and the most likely source of seismic radiation during the mainshock (Ammon et al 1994; Arvidsson et al 2002; Li and Toksöz 1993) came from a region consistent with the location of rectangle 4; B) rupture during both the precursory and mainshock concentrated at the center of the faults, at depths between 6.6 and 13.3 km, corresponding to the location of rectangle 5 (see Fig. 4).

3 Results

3.1 Analysis of earthquake catalog

We used a total of 1703 shallow earthquakes with $0.7 \leq M_L \leq 6.1$ detected by RSNC during June 1993 – September 2007. During this period we found changes in the reported seismicity which could represent actual variations in seismicity rates or changes in the detection level. Three major changes or periods, named I (oldest), II, and III (the most recent), are clearly seen in a plot of cumulative number of earthquakes versus time (Fig. 2). A motivation for this study was the apparent increase in seismicity in the region starting in early 2003 and the intermediate-term variability in seismicity within period III (2003–2007) (Dionicio 2008). A plot of the magnitude of completeness (M_C) versus time revealed variability in the level of complete detection between 1993 and 1997, relative stability until 2003 and again variability

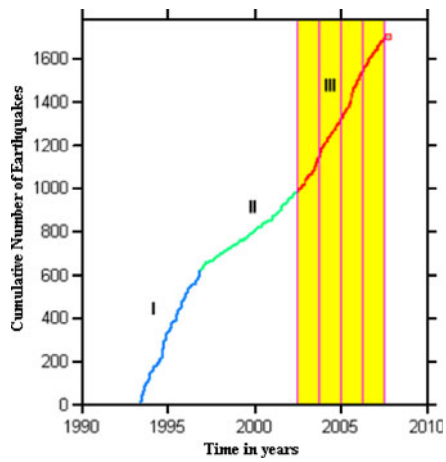

Fig. 2 Plot of cumulative number of earthquakes versus time. Periods with different rate of seismicity are marked by different colors and labeled I, II, and III. Within period III we highlight the period 2003–2007 with yellow and vertical red lines are yearly tick lines.

thereafter. During the period of interest (III), although M_C shows increases and decreases during 2003–2007, these variations are generally in sync with variations in seismicity rates (i.e. when M_C rises seismicity increases). This indicates that the changes in seismicity rate are not artificial. M_C varies between 2.6 and 3 during 1993 and 2007.

The frequency-magnitude distribution, FMD, during 1993–2007 indicates $M_C = 2.7$ for the entire catalog and the slope of the best-fitting line to data above M_C represents an average b-value of 0.75 (Fig. 3). We analyzed the spatial distribution of b-values by measuring b for the n = 100 earthquakes nearest to each node of a 1×1 km grid. The b-value computed for each sample is color-coded and the results are shown in Fig. 3. We observed that within the study region $0.6 \leq b \leq 2.0$ and those b-values are relatively low to the NW and central areas and relatively high to the south. These results do not vary when mapping b using alternative methods.

3.2 Earthquakes relocation

We relocated 595 epicenters detected by RSNC during 1993–2007. The results are shown in Fig. 1. After relocation epicenters seem to concentrate into two main groups, one is an N-S alignment west of the Murindó fault and the other is a clustering east of the Murrí fault, with some SE-NW elongation. The relocation procedure did not change significantly the depths of earthquakes, probably because there are not nearby seismograph stations.

The Murindó fault has been described either as an east-dipping structure (Paris et al 2000) or a vertical strike-slip fault with left-lateral motion (Gómez et al 2007), one would expect its associated seismicity to concentrate east of the surface trace. Our results, however, indicate that most of seismicity (both original and relocated earthquakes) may not be occurring as a result of slip on the Murindó fault. Alternatively, it is

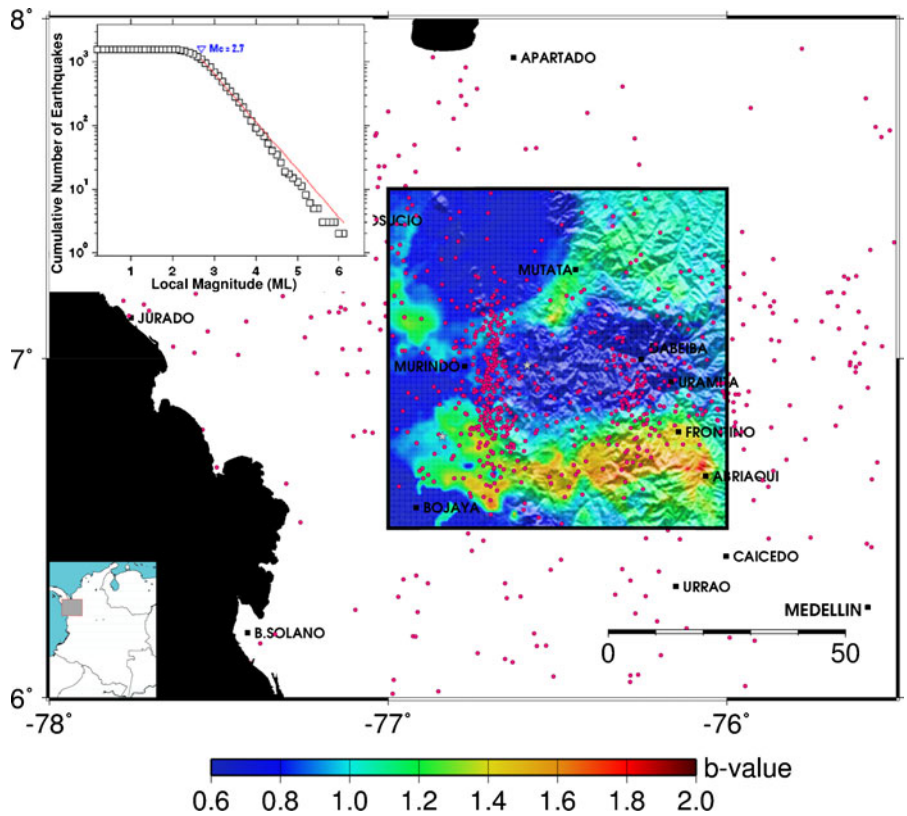

Fig. 3 Map of b-values. A 1 km × 1 km grid was used to select the nearest $n = 100$ epicenters around each node. Colors indicate relatively high (red) or relatively low (blue) b-values. Inset: The frequency-magnitude distribution for the 1993–2006 preliminary dataset. An inverted triangle marks an estimate of the magnitude of completeness $M_C = 2.7$. Other conventions as in Fig. 1.

also plausible that the Murindó fault is actually dipping to the west. We also note that the original JHD relocations by Arvidsson et al (2002) for the 1992 sequence and aftershocks would also not be associated with the Murindó fault.

3.3 Static stress changes during the entire 1992 sequence

We computed Coulomb stress changes imparted by the precursory earthquake on specific faults with orientation similar to the mainshock fault (strike $= 9°$, dip $= 81°$, slip $= 46°$) for a target depth of 15 km. The distribution of slip within the model fault is as described in test A of Table 4, Fig. 4. For all tests we found a similar behavior: A lobed pattern of alternating positive and negative regions of stress change surrounding the fault. The epicenter of the mainshock of October 18 falls within a zone of positive stress changes. In the vertical cross-section near the northern tip of the model fault we see that the fault plane appears

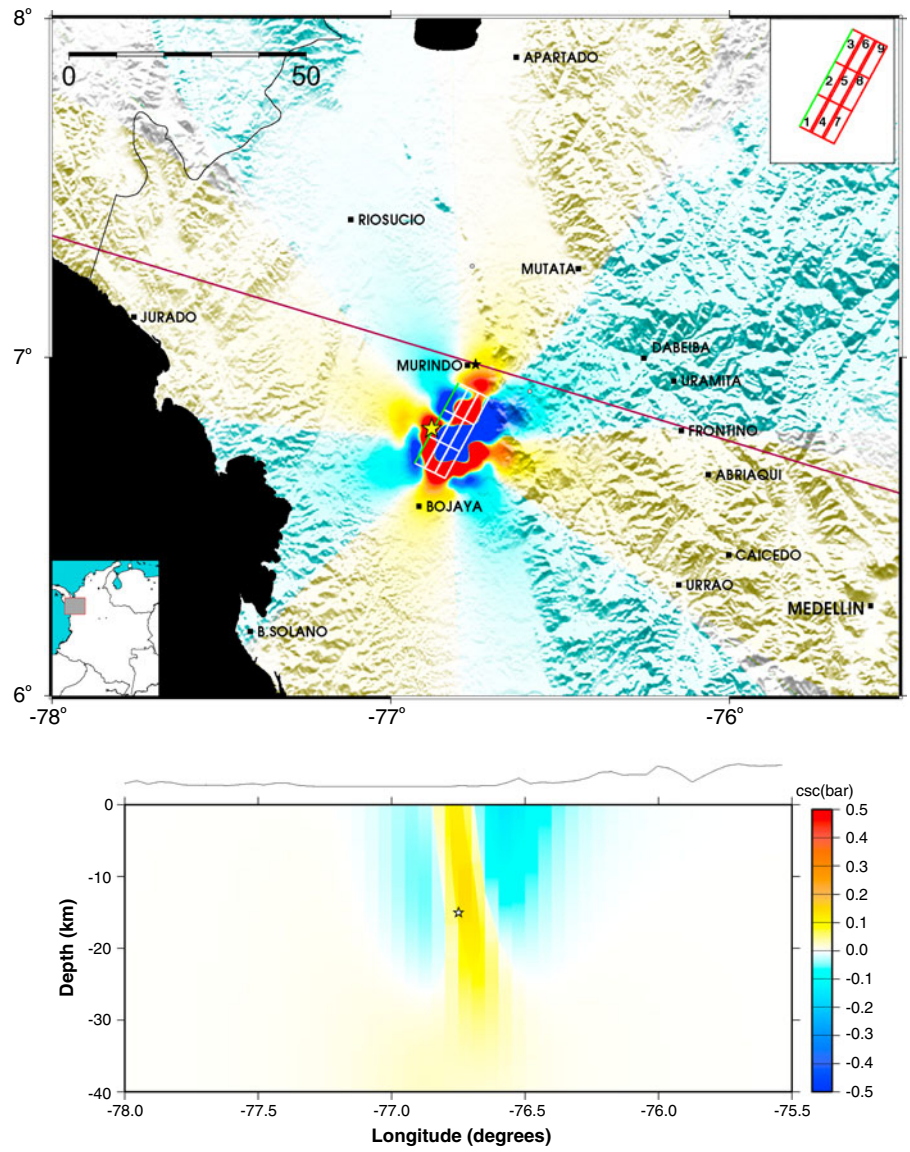

Fig. 4 Top: Coulomb stress changes during the $M_W = 6.6$ earthquake on October 17, 1992 (yellow start), calculated on specifically oriented faults (strike $= 9°$, dip $= 81°$, slip $= 46°$, target depth $=$ 15 km). White rectangle: model fault (green line shows surface projection of fault). Black star: Epicenter of mainshock on October 18, 1992. The fault is subdivided into nine smaller rectangles where slip was assigned to model different scenarios (see "Test B" in Table 4), the numeration of the rectangles is shown in the top right-hand corner. Black squares: Towns and villages. Purple line: Orientation and length of vertical cross-section shown at the bottom of the figure.

surrounded entirely by positive stress changes and that two regions of negative stress changes locate to either side of the fault.

We also computed Coulomb stress changes imparted by the entire 1992 sequence on optimally-oriented strike-slip faults at a target depth of 7.5 km, using the distribution of slip indicated in test A of Table 4, the modeling of cumulative stress changes as produced by localized slip in the central patch (precursory fault) and southern patch (main fault) shows results (Fig. 5) consistent with alternative models of uniform slip and tapered slip. When stress changes are projected onto specific faults in the area the results do not vary significantly compared to alternative models as well. For all tests we found a similar configuration of stress changes. The large values of stress change near the faults decay to low values

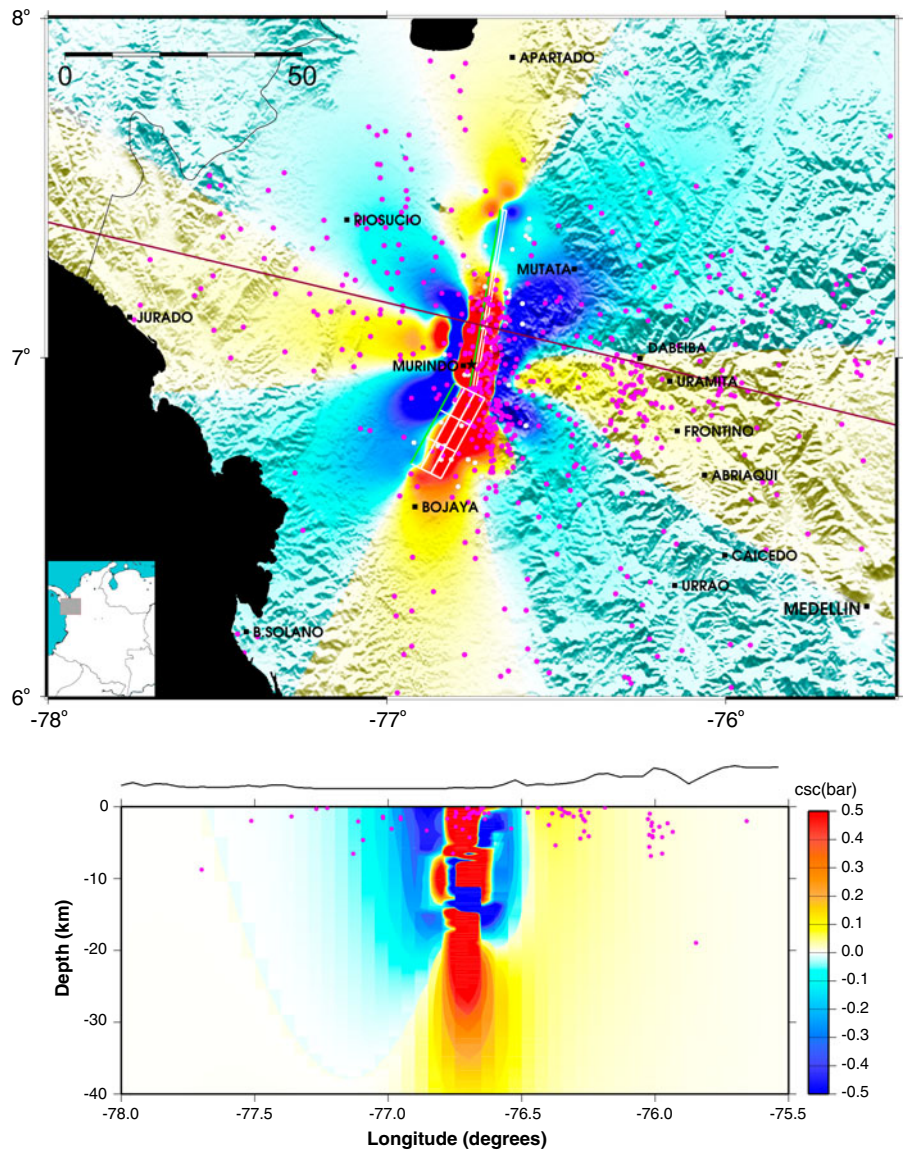

Fig. 5 Top: Coulomb stress changes produced by rupture during both events (precursory and mainshock) on October 17–18, 1992, projected on optimally oriented strike-slip faults. Target depth is 7.5 km. White and red circles: epicenters of relocated aftershocks (Arvidsson et al 2002) and relocated local seismicity respectively. Other conventions as in Fig. 4.

within 10 km. The lobes of negative stress changes occupy larger areas, compared to lobes of positive change.

Many of the aftershocks are explained by positive stress changes and part of the relocated background seismicity (1993–2006) shows a tendency to occur on positive lobes located to the south and east, at distances of over 60 km from the faults. The southern and eastern lobes of positive stress changes are a preferential zone for background seismicity, compared to the northern lobe.

3.3.1 Nearby faults in the region

We also computed Coulomb stress changes imparted on various faults in the region.

An interesting result of our analysis concerns the Murindó fault, as mapped by Gómez et al (2007). While the central segment falls completely within a zone of negative stress changes, the northern segment is almost entirely within a zone of strong positive changes (see Fig. 6). The implication is that the 1992 sequence could potentially simultaneously alter in different ways the seismic cycle for this important fault. The central segment may have been delayed but the northern segment could have been taken closer to rupture.

For the Murrí fault we see that the north and south ends fall within areas of negative stress change, giving a "clamping" effect that would inhibit rupture. The central segment falls in a zone if positive stress changes. For Mutatá fault the northwest end of the fault falls in a region of positive stress change (~ 0.1 bar), which indicate that rupture would be facilitated in those areas of the fault, bud the rest of the fault is affected by negative stress changes. The Urrao

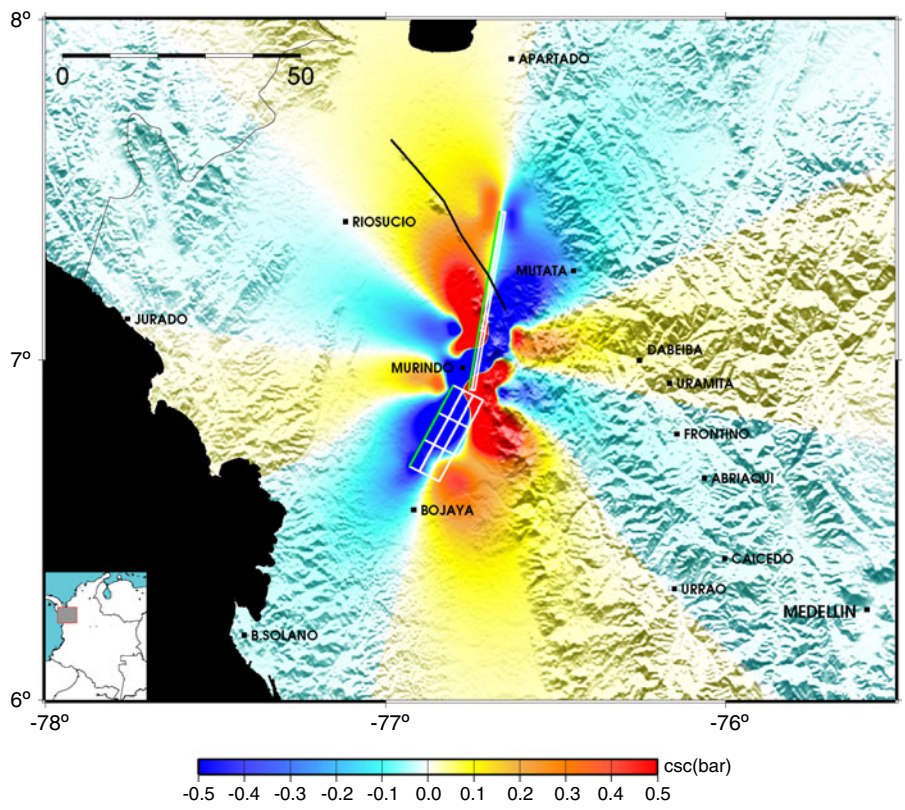

Fig. 6 Coulomb stress changes produced by the 1992 sequence, projected on the north segment of Murindó fault. Target depth is 7.5 km. Conventions as in Fig. 4.

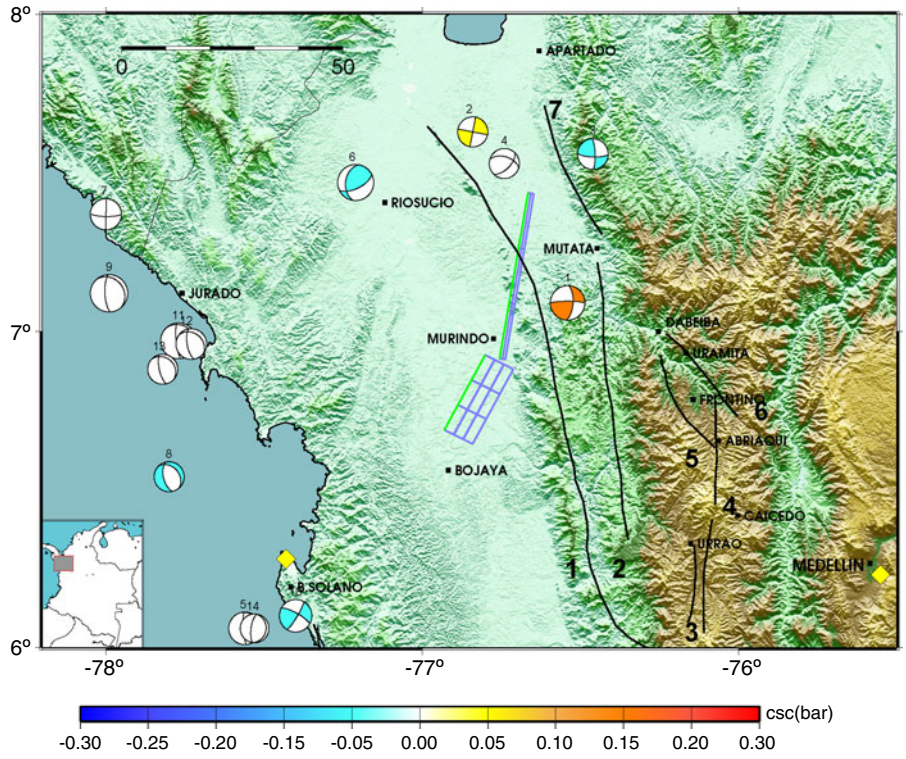

Fig. 7 Coulomb stress changes produced by the 1992 sequence, projected on specifically oriented faults as those with the focal mechanisms shown. The focal mechanisms are from GCMT and were computed for earthquakes with $M_W \geq 5.2$ during 1994–2008. Numbers correspond to those in Table 5. Conventions as in Fig. 4.

fault trace falls entirely on a region of negative stress changes of approximately 0.1 bar. For the Cañasgordas fault we observe that all the structure, except its southeastern end, is immersed in a zone of positive stress changes of roughly 0.02 bar.

Table 5 Earthquakes with $M_W \geq 5.2$ reported by GCMT during 1994–2008

N	Date	Time	Lat. (°)	Lon. (°)	Depth. (km)	M_w	ϕ (°)	δ (°)	λ (°)	Scalar Moment	csc (bars)
1	1994/09/13	10:01:39.0	7.09	−76.54	23.00	6.0	4	64	9	1.35e+25	0.14
2	1995/03/19	17:04:11.40	7.63	−76.84	15.40	5.2	281	90	−180	9.3e+23	0.01
3	1995/03/23	02:08:40.90	7.56	−76.46	15.40	5.4	358	78	17	1.37e+24	−0.02
4	1996/05/13	04:53:52.90	7.53	−76.74	33.80	5.2	287	52	139	8.79e+23	0.00
5	1996/05/23	05:23:26.90	6.06	−77.56	15.90	5.7	349	8	82	3.82e+24	0.00
6	1996/11/04	17:25:04.20	7.47	−77.21	15.00	6.3	188	43	42	3.05e+25	−0.03
7	1999/01/04	08:43:46.70	7.37	−78.00	17.20	5.4	91	78	−179	1.7e+24	0.00
8	2000/07/12	22:12:24.40	6.54	−77.80	15.00	5.2	319	34	−114	8.62e+23	−0.01
9	2000/11/08	07:00:15.70	7.12	−77.99	17.00	6.5	321	22	56	7.06e+25	0.00
10	2003/01/08	14:29:09.70	6.10	−77.40	25.10	5.7	299	76	172	3.79e+24	−0.01
11	2006/01/23	20:50:50.00	6.97	−77.77	15.00	6.2	316	14	53	2.73e+25	0.00
12	2006/01/24	02:15:48.10	6.96	−77.73	23.70	5.4	307	29	50	1.34e+24	0.00
13	2006/01/29	17:49:20.40	6.88	−77.82	27.00	5.2	313	23	58	8.15e+23	0.00
14	2007/09/22	11:44:43.20	6.06	−77.53	20.30	5.0	8	70	90	3.97e+23	0.00

3.3.2 Relationship between Coulomb stress changes from the 1992 sequence and seismicity $M_W \geq 5.2$ in the region

In Fig. 7 we show the computed Coulomb stress changes from the 1992 sequence imparted on specific faults represented by the nodal planes of focal mechanisms for earthquakes with $M_W \geq 5.2$ occurred between 1994 and 2008. These earthquakes and their fault plane solutions are taken from GCMT (2008) (Table 5). We see that moderate earthquakes possibly facilitated by the stress changes of the 1992 sequence locate to the east and north of our model faults. Their fault plane solutions are consistent with movement along left-lateral strike-slip faults. Earthquakes located west of the model faults would not have been affected or would have been slightly inhibited by the 1992 sequence. Their mechanisms correspond to reverse faults. The results described do not change when a fault model with tapered slip is used.

4 Discussion

4.1 Analysis of the earthquake catalog

We analyzed the seismicity detected by RSNC during 1993–2006 to determine the magnitude of completeness (M_C) and the average b-values. We found the RSNC catalog to be complete down to $M_C = 2.7$, and using this as a minimum magnitude we found an average of $b = 0.8$. The mapping of b-values over the study region shows relatively low values in the central, western, and northwestern areas and relatively high values in a restricted zone to the south-southeast (Fig. 3). Most of the background seismicity clearly occurs in areas of low b-values, indicating a large region of stress concentration, apt for the occurrence of relatively larger shocks. The region were the 1992 sequence nucleated was clearly under a large stress load, and from the spatial distribution of b-values after 1993 it appears as if mostly a belt-shaped area to the south of the study region was under relaxed conditions of stress, a rather intriguing result with possible hazard implications. Intuitively, the regions near the hypocenters of both the precursory and mainshock during the 1992 sequence should in the following years be relaxed regions. Our results of b-value mapping, however, indicate that during the following decade, most of the study region remains still under stress load, because on average, large earthquakes tend to occur. Only a restricted region of relatively high b-values to the south-southeast appears to have relaxed. The precursory earthquake on October 17, 1992, occurred in this area, but the mainshock nucleated farther north.

4.2 Earthquake relocation

The earthquake relocation give us a clearer picture of the spatial distribution of seismicity, which shows that there exist seismogenic zones attributable to mapped and unmapped faults in the region; as previously suggested Arvidsson et al (2002). A notable feature of the relocated earthquakes is the persistence of groups of epicenters east and west of the towns of Murindó and Dabeiba respectively, which have been repeatedly affected by shaking in the past years. It is possible that by using waveform cross-correlations the relocations can be improved, but this would constitute a separate study.

4.3 Definition of a model for the seismic source and Coulomb stress calculation

Based on the alignment of relocated aftershocks using JHD (Arvidsson et al 2002), reports of surface effects during the earthquakes (Martinez et al 1994), and the reported focal mechanisms for the 1992 earthquakes (GCMT 2008), we built various models for the configuration of the causative faults and the distribution of slip (Fig. 5, Table 4). In general we find an elaborate model using subdivided or tapered slip the fault surface explains the spatial distribution of aftershocks and subsequent background seismicity, and the possible facilitation or inhibition of rupture along nearby faults, the changes in Coulomb stress for these models are mainly in the range −0.5 to 0.5 bars, concordant with results for earthquake sequences elsewhere (Anderson and Ji 2003; Hreinsdöttir et al 2002). We suggest that a more realistic scenario may arise when combining features of the

various models. In particular we found that by using reasonable model parameters it is possible to postulate the character of the earthquake on October 17, 1992, as a facilitator of rupture nucleation for the mainshock on October 18. Also we found that, when projecting changes in stress on optimally-oriented strike-slip faults, we saw that along with well explained epicenters there is also a portion of the seismicity that falls in areas of negative Coulomb stress changes. A plausible explanation for this is that some of the seismic activity may occur on normal or reverse faults. Another relevant result of our study is the intriguing possibility that the 1992 seismic sequence could have occurred along an unmapped fault. This is supported by the fact that relocations obtained in previous work by Arvidsson et al (2002), reports of surface effects, and background seismicity are no explained by stress changes imparted from nearby mapped faults like Murindó or Murrí.

4.4 Implications for seismic hazard

Documented cases of seismic sequences around the world show that earthquakes produce static stress changes that in turn increase or decrease the likelihood of occurrence of rupture along nearby faults. It has been showed, for instance, how the occurrence of the 1992 Landers, California, earthquake may have been facilitated (and in fact advanced several centuries) by stress changes of $\sim$ 1 bar imparted by foreshocks. During the 2002 Denali, Alaska, seismic sequence it was determined that positive stress changes of 0.3–0.5 bars produced by an M_W6.7 foreshock facilitated the occurrence of a M_W7.9 mainshock 13 days later, and that the cumulative positive stress changes imparted to the region from both the foreshock and mainshock were in the range $0.8 - 4.0$ bars.

Our results of stress changes during the 1992 Murindó seismic sequence are consistent with those documented results and allow us to suggest that the stress state on important faults of the region may have been altered and that the possibility exists that some faults or fault segments in the area may have been prompted to rupture. The reach of our interpretations, however, is limited because of the lack of knowledge on previous earthquakes, paleoseismology, or stress state, for many faults in Colombia. We thus hope our results be useful to foster a variety of investigations on paleoseismology, neotectonics, seismicity and tectonics, and to motivate the installation of state-of-the-art seismic instruments in order to achieve a better understanding of potentially hazardous faults.

4.5 Suggestions for future work

The results presented contribute with valuable information on fault-to-fault interactions and the plausible effects of stress changes from earthquakes. At the same time we confront questions that can be tackled in future studies: **1)** In hindsight, is it possible to find other cases of earthquake interactions in Colombia? **2)** What was the order of static stress changes resulting from great earthquakes, such as the *Ms* 8.8 earthquake on the pacific coast of Colombia-Ecuador, on January 31st, 1906? **3)** In terms of earthquakes-volcanoes interactions, what possible scenarios exist so that volcanic activity may be influenced by rupture along nearby faults? Or vice versa? **4)** How can we integrate other Geophysical data, such as GPS, satellite interferometry, and paleoseismology with results, data, and models from seismology?

5 Conclusions

Based on the analysis of the RSNC earthquake catalog we conclude that $M_C = 2.7$ and $b = 0.8$, on average, for the study region. The mapping of b-values indicates relatively low b values ($b \sim 0.6$) for the central and northwest areas, and relatively high b ($b \sim 1.8$) to the south.

The Double Difference method of earthquake relocation is a powerful tool to constrain the spatial distribution of seismicity. We suggest that some relevant clusters of seismicity in the region can be attributable to unmapped faults. Our results can be improved by including waveform cross-correlation in future studies.

Our model supports the suggestion that the M_W6.6 foreshock on October 17, 1992, facilitated the relatively rapid occurrence of the M_W7.1 mainshock on October 18, 1992. By using various models for the distribution of slip along

precursory and main faults, we explain several characteristics of the distribution of aftershocks and background seismicity for the region. The results among models vary mostly in the spatial distribution and range of stress changes, but the key features of seismicity remain relatively well explained.

The Coulomb stress changes resulting from the 1992 seismic sequence may have accelerated or delayed the rupture of other relevant faults in the region. This has implications for seismic hazard, but much remains to be done. Future research endeavors and the integration of multidisciplinary studies are key in solving important questions.

Acknowledgements We are indebted to L. F. Castillo and E. Franco for their valuable help during the early stages of this study. We thank INGEOMINAS and RSNC for allowing us to use their seismicity data. We are grateful to all the RSNC staff involved in data management, deployment, and maintenance of seismic stations.

References

Ammon C, Lay T, Velasco A, Vidale J (1994) Routine estimation of earthquake source complexity: the 18 October 1992 Colombian earthquake. Bull Seismol Soc Am 84(4):1266–1271

Anderson G and Ji C (2003) Static stress transfer during the 2002 Nenana mountain-denali fault, Alaska, earthquake sequence. Geophys Res Lett 30:1310

Arvidsson R, Toral Boutet J, Kulhanek O (2002) Foreshocks and aftershocks of the $m_w = 7.1$, 1992, earthquake in the Atrato region, Colombia. J Seismol 6: 1–11

Cardona C, Salcedo E, Mora H (2005) Caracterización sismotectónica y geodinámica de la fuente sismogénica de Murindó - Colombia. Bol Geol 27(1):115–132

GCMT (2008) The global centroid-moment-tensor (gcmt) project. http://www.globalcmt.org

Cortés M and Angelier J (2005) Current states of stress in the northern Andes as indicated by focal mechanisms of earthquakes. Tectonophysics 403:29–58

Dewey J (1971) Seismicity studies with the method of jointhypocenter determination. PhD thesis, University of California, Berkley

Dionicio V (2008) Estudio y modelamiento de procesos sísmicos en el área de Murindó-Antioquia, e implicaciones en la amenaza sísmica. Master's thesis, Universidad Nacional de Colombia, Bogotá-Colombia

Duque-Caro H (1990) The choco block in the northwestern corner of South America: Structural, tectonostratigraphic, and paleogeographic implications. J South Am Earth Sci 3(1):71–84

Gómez J, Nivia A, Guevara A, Montes N, Jiménez D, Sepúlveda M, Gaona T, Osorio J, Diederix H, Penagos M, Velásquez M (2007) Atlas geológico de Colombia. INGEOMINAS. Plancha 5-05

Havskov J and Ottemöller L (2005) Seisan: The earthquake analysis software. Department of Earth Science, University of Bergen. Version 8.1

Hreinsdöttir S, Fletcher H, Larsen C, Freymueller J (2002) Coseismic displacements from the m_w 6.7 and m_w 7.9 Denali fault earthquakes and resulting coulomb stress change on faults in Alaska. Eos Trans AGU 83(47):S72F–1368

Li Y and Toksöz N (1993) Study of the source process of the 1992 colombia $m_s = 7.3$ earthquake with the empirical green's function method. Geophys Res Lett 20(11):1087–1090

Lin J, Ross S, Sevilgen V, S T (2000) Usgs-whoi-dpri coulomb stress-transfer model for the January 12, 2010, mw=7.0 Haiti earthquake. Open-File Report 2010–1019

Lin J and Stein R (2004) Stress triggering in thrust and subduction earthquakes and stress interaction between the southern San Andreas and nearby thrust and strike-slip faults. Geophys Res Lett 109:19

Martinez J, Parra E, Paris G, Forero C, Bustamante M, Cardona O, Jaramillo J (1994) Los sismos del Atrato medio 17 y 18 de Octubre de 1992 noroccidente de Colombia. Revista INGEOMINAS 4:35–76

Ojeda A and Havskov J (2001) Crustal structure and local seismicity in Colombia. J Seismol 5:575–593

Paris G, Machette M, Dart R, Haller K (2000) Map and database of quaternary faults and folds in Colombia and its offshore regions. Open-File Report 00-0284

Pulido N (2003) Seismotectonics of the northern Andes (Colombia) and the development of seismic networks. Bull Int Inst Seismol Earthq Eng 69–76. Special Edition

Stein S and Wysession M (2003) An introduction to seismology, earthquakes, and earth structure. Blackwell Publishing Ltd

Taboada A, Rivera L, Fuenzalida A, Cisternas A, Philip H, Bijwaard H, Olaya J, Rivera C (2000) Geodynamics of the northern andes: Subductions and intracontinental deformation (Colombia). Tectonophysics 19(5):787–813

Toda S, Stein R, Richards-Dinger K, Bozkurt S (2005) Forecasting the evolution of seismicity in southern California: animations built on earthquake stress transfer. Geophys Res Lett 110:17

Waldhauser F (2001) HypoDD - A program to compute Double-Difference Hypocenter Locations. U.S. Geological Survey. Open File Report 01–113

Waldhauser F and Ellsworth W (2000) A double-difference earthquake location algorithm: Method and application to the northern Hayward fault, California. Bull Seismol Soc Am 90(6):1353–1368

Wiemer S (2001) A software package to analyze seismicity: Zmap. Seismol Res Lett 72:373–382